Title

Fabrication of dislocation-free tensile strained Si thin films using controllably oxidized porous Si substrates

Journal

Applied Physics Letters, 89(15)

ISSN

0003-6951

Authors

Kim, J
Xie, Y H

Publication Date

2006-10-01

Peer reviewed

Fabrication of dislocation-free tensile strained Si thin films using controllably oxidized porous Si substrates

Jeehwan Kim[a] and Ya-Hong Xie
Department of Materials Science and Engineering, University of California at Los Angeles, Box 951595, Los Angeles, California 90095-1595

(Received 15 June 2006; accepted 30 August 2006; published online 12 October 2006)

A method to fabricate strained Si films is reported via the oxidation of a thin Si film on a porous Si substrate. The Si film can be put under tensile stress in a controllable fashion through the expansion of the porous Si upon low temperature oxidation. The thin Si layer on porous Si substrate can be fabricated using a self-limiting anodization of epitaxially grown intrinsic Si on a heavily doped *p*-type Si substrate. Tensile strain of up to ~1% is observed in 100 nm thick Si films, making it suitable for the various device applications based on strained Si. © *2006 American Institute of Physics*. [DOI: 10.1063/1.2360930]

Strained Si has been used for high electron mobility microelectronic device applications. Research on high mobility strained Si technologies has focused on lowering dislocation density and achieving uniform strain and flat surface morphology. More recently, process induced, locally strained Si technology has been introduced that has the distinct advantage in the manufacturability and has been incorporated in production. Both tensile and compressive strained Si layers have been fabricated as the channel layer for high speed field-effect transistors (FETs).[1,2] This process-induced local strain method is only applicable to nanoscale dimensions, which is ideal for the state-of-the-art FETs. For quantum transport studies [i.e., two-dimensional electron system (2DES)] on the other hand, the lateral device dimension needs to be hundreds of microns in order to avoid asymmetric Hall plateaus due to the filling of respective Landau levels.[3] Consequently, global strain is the only viable approach.

Different methods have been used for fabricating globally strained Si. The original approach involves growing a completely relaxed SiGe buffer layer through compositional grading during epitaxial growth. This approach reduces the density of threading dislocations from the typical $10^8/\mathrm{cm}^2-10^9/\mathrm{cm}^2$ in a uniform SiGe layer epitaxially grown on Si (001) substrate to about $10^4/\mathrm{cm}^2-10^5/\mathrm{cm}^2$.[4,5] Alternatively, Hobart *et al.* demonstrated a method for fabricating fully relaxed SiGe buffer layers without dislocations by relaxation of a fully strained SiGe film on top of a borophosphorosilicate glass (BPSG) layer at above the glass flow temperature of ~800 °C.[6,7] Using this method, uniform strain can be obtained only for SiGe films of small lateral dimension (typically $<100\ \mu$m). Moreover, the high concentration ($10^{21}-10^{22}\ \mathrm{cm}^{-3}$) of boron and phosphorus in BPSG causes outdiffusion during prolonged annealing of BPSG above glass flow temperatures, which is of serious concern for device applications as well as electron transport studies.

In this letter, we introduce a process using the oxidation of a thin film Si on a porous substrate for fabricating high quality strained Si films with global tensile strain. No misfit dislocation is ever introduced into the structure throughout the entire fabrication process, leading to strain homogeneity in the Si film. Moreover, this method does not require patterning of the Si film.

Intrinsic Si layers of various thicknesses (100–500 nm) are grown on top of the heavily doped *p*-type substrate using a Riber EVA-32 molecular-beam epitaxy system. Si wafers used are heavily doped (100) *p*-type single crystals ($\rho = 0.001-0.005\ \Omega\,\mathrm{cm}$). The anodization to fabricate a microporous Si is performed for 4 h with a current density of $50\ \mathrm{mA/cm}^2$ in an electrolyte composed of 1:1 volume ratio of HF (49%) to ethanol. The Si wafer is biased as an anode with the backside of the wafer (the opposite side of the epitaxial Si layer) being in contact with the electrolyte and a platinum foil as a cathode. One of the key elements to this approach is that the anodization comes to a nearly complete stop when the anodization front reaches the intrinsic Si layer. The cessation of anodization is associated with a noticeable change in the anodization voltage. The complete anodization of the heavily doped *p*-type substrate upon adequate overetch and the effectiveness of the etch stop (the intrinsic layer) are verified using a cross-sectional scanning electron microscope (SEM) (Hitachi S4700 field emission SEM). The surfaces of the as-anodized samples show a significant degree of roughness. A chemical mechanical polishing in a Logitech chemical, delayering, and planarization polishing system is used to recover a surface flatness to ±0.4 nm.

The anodized samples are oxidized at 500 °C in a steam ambient with 20 SCCM O_2 (SCCM denotes cubic centimeter per minute at STP) flowing through the boiling de-ionized

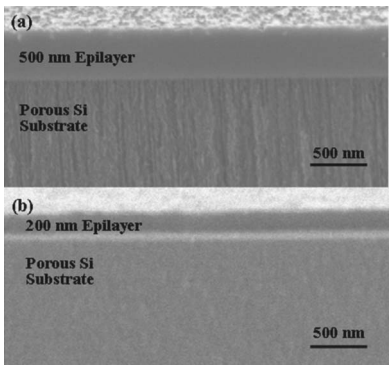

FIG. 1. Cross-sectional SEM images of (a) a 500 nm thick Si on porous Si substrate, and (b) a 200 nm thick Si on porous Si substrate.

[a]Electronic mail: jhkim03@ucla.edu

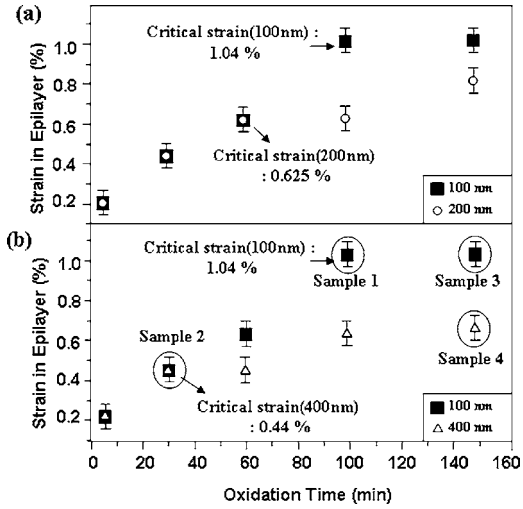

FIG. 2. Strain in the thin Si films as a function of oxidation time. (a) The 100 and 200 nm thick Si films, and (b) the 100 and 400 nm thick Si films.

water. Biaxial strain in the thin Si layers is measured using a Renishaw microscope Raman spectrometer. The laser penetration depth of the Raman measurement is approximately 200 nm. The Raman peak position shift is dependent on the strain[8] according to

$$\omega_{\mathrm{Si-Si}} = 521 - 815\varepsilon(\mathrm{cm}^{-1}), \tag{1}$$

where $\omega_{\mathrm{Si-Si}}$ is the angular frequency of the optical phonons in Si and ε is the strain in the Si epilayer. In order to verify the absence of dislocation in the strained Si layer, the chemical defect etch technique using a diluted Schimmel etchant (1 part $0.3M$ CrO_3, 1 part 49% HF, and 1 part DI water) is employed.

Figures 1(a) and 1(b) show the cross-sectional SEM images of the porous-crystalline interfaces of substrates that have been anodized for 4 h. It is evident that the thickness of the intrinsic epilayers remains significantly unchanged from that of the epitaxially grown films of 500 and 200 nm, respectively, which demonstrates the effectiveness of the intrinsic Si as an etch stop layer.

Figure 2 shows the dependence of strain in the thin Si film on the oxidation time. The strain is seen to increase linearly with increasing oxidation time until it reaches saturation at a critical value. We consider the universal behavior of films of various thicknesses for short oxidation times to be a result of the fact that they are fully strained. The critical strain value is higher for thinner Si layers, being approximately 1.0%, 0.6%, and 0.4% for the Si layers of 100, 200, and 400 nm, respectively. Even after the strain saturation, the strain appears to increase slightly for long oxidation times. While the reason is currently not certain, we speculate that such behavior is likely to be due to the imbalance between the relaxation rate and the strain loading rate from continued oxidation of porous Si. Similar behavior of film thickness dependence was observed for SiGe films epitaxially grown on Si (001) by Bean *et al.* who identified the critical thickness as the thickness above which the kinetically limited introduction of dislocations becomes measurable.[9] Considering the tensile nature of the strained thin Si layers, the observed strain saturation may be the result of crack formation or a combination of dislocation and crack formation.[10–12] We performed defect etch on the samples before and after strain relaxation. For the samples with 100 and 400 nm Si thickness [marked as sample 1 and sample 2, respectively in Fig. 2(b)] oxidized right before strain saturation, cracks and etch pits are absent under both the optical microscope and SEM. This result clearly indicates that the layers whose strains are in the linear regime in Fig. 2 have neither dislocation nor crack. On the other hand, Figs. 3(a) and 3(b) show that there are cracks but not etch pits in the 100 nm Si layer oxidized for 150 min (sample 3), which is during the early stage of relaxation. This allows us to postulate that critical strain for cracking (ε_c) is smaller than that for dislocation introduction (ε_d). Murray *et al.* formulate the critical thickness for cracking assuming no preexisting cracks as follows:[10]

$$t_c = \frac{\gamma(1-\nu)}{G(1+\nu)f^2}, \tag{2}$$

where γ is the surface energy of the crack plane, ν is Poisson's ratio, f is misfit strain, and G is the shear modulus of the epilayer. Inserting the physical parameters for Si into Eq. (2) leads to the critical Si film thickness for crack formation,

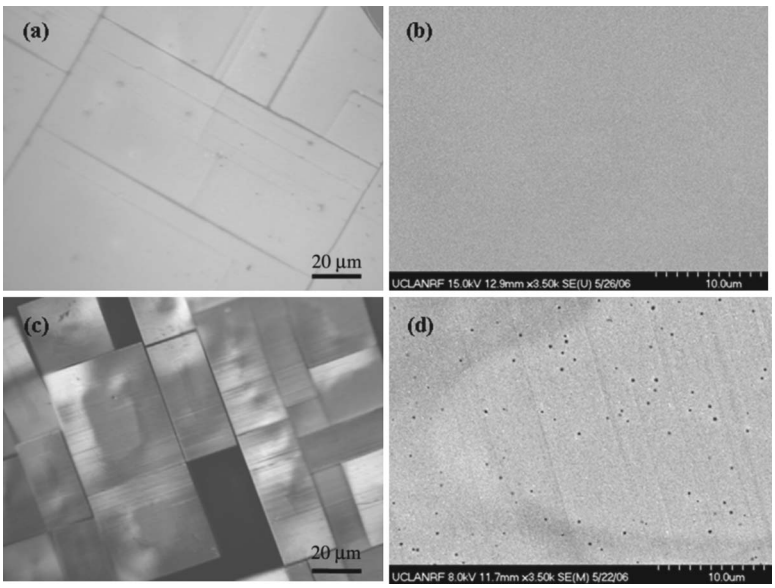

FIG. 3. Plan-view micrographs from relaxed layers after defect etch. (a) The Nomarsky interference micrograph of the 100 nm thick Si (sample 3) and (b) the SEM micrograph of the 100 nm thick Si (sample 3). (c) The Nomarsky interference micrograph of the 400 nm thick Si (sample 4) and (d) the SEM micrograph of the 400 nm thick Si (sample 4).

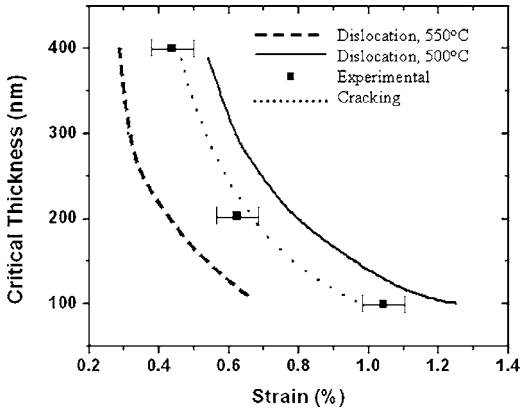

FIG. 4. Theoretical and experimental critical thicknesses for dislocation introduction (Ref. 13) and crack formation (Ref. 10).

$$t_c = 0.0107 f^{-2}(\text{nm}). \quad (3)$$

In Fig. 4, we plot this together with kinetically modified critical thickness for dislocation introduction[13] as well as our experimental results. The figure shows that ε_c is smaller than ε_d throughout the thickness range studied. In addition, our experimental results agree well with the theoretically derived ε_c, indicating that under our experimental condition crack formation precedes misfit dislocation introduction. Considering both crack formation and dislocation introduction are most likely dominated by heterogeneous mechanisms, such excellent agreement between the theoretical model and the experimental results is possibly fortuitous. However, the important point demonstrated by our experimental result is that the critical strain for cracking is lower than that for dislocation, as predicted by theory. For thicker films (e.g., sample 4 with 400 nm Si thickness) whose misfit and residual strains are higher than critical strain for dislocation introduction, Figs. 3(c) and 3(d) show clear signs of both cracks as well as dislocations (as evidenced by the presence of etch pits). The dark black area at Fig. 3(c) is caused by the infiltration of Schimmel etchant into the interface between the Si film and porous Si leading to local delamination. The strain is confirmed via multiple strain measurements across the fully strained 100 nm sample showing that the strain is uniform within the experimental uncertainty (<1 cm^{-1}) of the Raman technique.[14]

Another important feature of Fig. 2 is the linear dependence of the universal portion of the strain versus oxidation time curves for the Si films of different thickness. The linear behavior is an indication that the lateral (in-plane) strain in the oxidized porous Si is linearly proportional to the SiO_2 thickness on the pore walls because our oxidation process at 500 °C is indeed in the linear regime as opposed to the parabolic regime.[15]

It should be pointed out that the maximum achievable strain is limited by the Si film thickness. Fabricating Si/porous Si bilayer structures with Si film thickness significantly less than 100 nm value will be challenging in practice, but will lead to higher level of coherent strain.

In summary, we report a method for fabricating dislocation-free strained Si with the objective of achieving unprecedented level of strain homogeneity for electron transport studies. We employ a self-limiting process to fabricate thin Si films as thin as 100 nm on microporous Si substrate. Low temperature oxidation of the porous Si substrate results in thin Si film being strained to as high as 1%, comparable to that in a Si film epitaxially grown on a relaxed SiGe buffer layer of 25% Ge content. It is a significant step forward in sample fabrication for transport physics research into 2DES under extreme conditions and potentially for FETs applications.

The authors would like to thank Kang Wang of UCLA and his students for their help in Raman measurements. The research is supported in part by AFOSR (No. FA9550-04-1-0370, Donald Silversmith).

[1] S. Thompson, M. Armstrong, C. Auth, M. Alavi, M. Buehler, R. Chau, S. Cea, T. Ghani, G. Glass, T. Hoffman, C. Jan, C. Kenyon, J. Klaus, K. Kuhn, Z. Ma, B. Mcintyre, K. Mistry, A. Murthy, B. Obradovic, R. Nagisetty, P. Nguyen, S. Sivakumar, R. Shaheed, L. Shifren, B. Tufts, S. Tyagi, M. Bohr, and Y. El-Mansy, IEEE Trans. Electron Devices **51**, 1790 (2004).
[2] S. Thompson, M. Armstrong, C. Auth, S. Cea, R. Chau, G. Glass, T. Hoffman, J. Klaus, Z. Ma, B. Mcintyre, A. Murthy, B. Obradovic, L. Shifren, S. Sivakumar, S. Tyagi, T. Ghani, K. Mistry, M. Bohr, and Y. El-Mansy, IEEE Electron Device Lett. **25**, 191 (2004).
[3] H. Z. Zheng, K. K. Choi, D. C. Tsui, and G. Weimann, Phys. Rev. Lett. **55**, 1144 (1985).
[4] E. A. Fitzgerald, Y. H. Xie, M. L. Green, D. Brasen, A. R. Kortan, J. Michel, Y.-J. Mii, and B. E. Weir, Appl. Phys. Lett. **59**, 811 (1991).
[5] J. Jung, M. L. Lee, E. A. Fitzgerald, and D. Antoniadis, IEEE Electron Device Lett. **24**, 460 (2003).
[6] K. D. Hobart, F. J. Kub, M. Fatemi, M. E. Twigg, P. E. Thompson, T. S. Kuan, and C. K. Inoki, J. Electron. Mater. **29**, 897 (2000).
[7] H. Yin, R. Huang, K. D. Hobart, Z. Suo, T. S. Kuan, C. K. Inoki, S. R. Shieh, T. S. Duffy, F. J. Kub, and J. C. Sturm, J. Appl. Phys. **91**, 9716 (2002).
[8] J. C. Tsang, P. M. Mooney, F. Dacol, and J. O. Chu, J. Appl. Phys. **75**, 8098 (1994).
[9] J. C. Bean, L. C. Feldman, A. T. Fiory, S. Nakahara, and I. K. Robinson, J. Vac. Sci. Technol. A **2**, 436 (1984).
[10] R. T. Murray, C. J. Kiely, and M. Hopkinson, Philos. Mag. A **74**, 383 (1996).
[11] P. Maigné, M. Gendry, T. Venet, Y. Tahri, and G. Hollinger, Appl. Phys. Lett. **69**, 682 (1996).
[12] M. Natali, D. De Salvador, M. Berti, A. V. Drigo, L. Lazzarini, G. Salviati, G. Rossetto, and G. Torzo, J. Vac. Sci. Technol. B **18**, 2527 (2000).
[13] D. C. Houghton, J. Appl. Phys. **70**, 2136 (1991).
[14] W. Trzeciakowski, J. Martínez-Pastor, and A. Cantarero, J. Appl. Phys. **82**, 3976 (1997).
[15] S. M. Hu, J. Appl. Phys. **57**, 4527 (1985).